View metadata, citation and similar papers at core.ac.uk

brought to you by CORE

provided by Elsevier - Publisher Connector

produced for each patient. All plans had a mean CTV dose of 18.75 Gy per fraction (=100% dose) and 95% minimum CTV dose coverage. The PTV was covered by 50%, 67%_S, 67% (our standard), 80%, and 95% of the prescribed dose, respectively. The 67%_S plan was an alternative to the standard 67% plan made with maximum conformity, i.e. as steep as possible dose gradient from 95% to 67% outside the CTV. The 50%, 67%_S, 80%, and 95% plans were renormalized to be isotoxic with the standard 67% plan, i.e. to give the same risk of radiation induced liver disease (RILD) according to the NTCP-model of Dawson *et al*. (Acta Oncol., 2006). For each patient and plan, the dosimetric effects of the observed intrafraction motion were investigated by calculating the delivered dose by an in-house developed method for motion-including dose reconstruction.

Results: The figure shows the CTV mean dose and D99 for each plan type and each patient as planned (start of each arrow) and as delivered with the known tumor motion (end of each arrow). The mean values over all patients are presented in Table 1. The planned CTV dose decreased markedly from 63.3Gy to 47.0Gy (average mean dose) and from 60.5Gy to 44.9Gy (average D99) as the prescription level to the PTV rim was increased from 50% to 95%. Although intrafraction motion reduced this CTV dose difference the CTV dose of plans with high PTV prescription levels remained inferior to isotoxic plans with low PTV prescription levels even when motion was included in the dose calculations, see Table 1. The absolute dose delivered to the liver was almost unaffected by intrafraction motion as seen in Table 1.

Figure 1

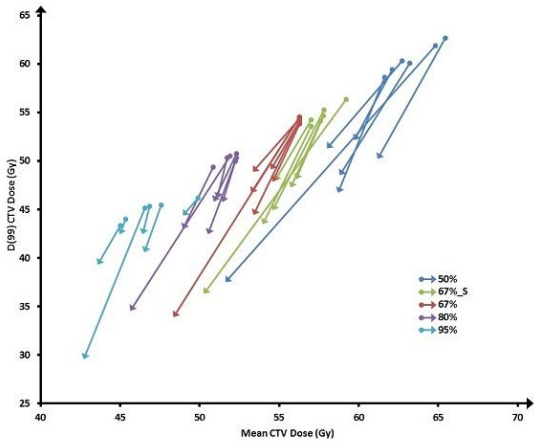

Mean dose (horizontal axis) and D99 (vertical axis) for CTV for each plan type for each patient as planned (start of each arrow) and as delivered with the known tumor motion (end of each arrow). Each color represent a plan type.

Conclusion: The dose level at the PTV rim has a large effect on the risk of RILD. Using a low dose at the PTV rim, where the probability of CTV presence during treatment was low, allowed for higher CTV dose for iso-toxic conditions in 50% and 67%_S plans. Although these plans were less robust to intra-fraction motion, their CTV dose remained superior to the 80% and 95% plans when motion effects were included.

Table 1

PTV prescription dose	Planned mean CTV dose (Gy)	Delivered mean CTV dose (Gy)	Planned mean CTV D_{99} dose (Gy)	Delivered mean CTV D_{99} dose (Gy)	Planned mean liver dose (Gy)	Delivered mean liver dose (Gy)
50%	63.3	58.0	60.5	47.8	10.91	10.53
67%_S	57.7	54.2	54.7	44.7	11.03	10.80
67%	56.3	52.9	54.3	45.5	10.97	10.66
80%	52.0	49.7	50.2	43.0	11.05	10.72
95%	47.0	45.5	44.9	39.8	11.13	10.93

PO-0891

Clinical implementation and experience with real-time anatomy tracking and gating during MR-IGRT

O. Green[1], L. Rankine[2], L. Santanam[1], R. Kashani[1], C. Robinson[1], P. Parikh[1], J. Bradley[1], J. Olsen[1], S. Mutic[1]

[1]*Washington University School of Medicine, Radiation Oncology, St. Louis, USA*

[2]*University of North Carolina, Radiation Oncology, Chapel Hill, USA*

Purpose or Objective: To describe the commissioning process and initial experience using real-anatomy, real-time tracking and gating with MRI-guided radiation therapy.

Material and Methods: An MR-IGRT system was commissioned to enable real-time anatomy tracking and gating. The imaging rate is 4 frames per second; the radiation shuts off when the anatomy of interest is automatically detected outside a pre-defined treatment region. The specific commissioning tests were driven by the goal of compensating for the inherent system latency such that there would not be an increase in treatment margins (i.e., GTV to PTV expansion). Dosimetric and geometric accuracy was evaluated by using both a commercial and an in-house motion phantoms with film and ionization chamber dosimetry. Clinical procedures were developed to maintain the established accuracy during actual patient treatments.

Results: Since initial clinical implementation, 51 patients have been treated using the gating and tracking capability of the MR-IGRT system (out of a total of 193). Based on system characteristics established during commissioning tests, the standard-of-care GTV to PTV expansion was maintained (e.g., 5 mm for abdominal tumors). Dosimetric accuracy was established via ionization chamber measurements that showed a 1.28%±1.7% average difference when comparing gated (with motion) vs. non-gated (without motion) delivery for typical IMRT and open field plans. Spatial accuracy was established via film dosimetric measurements and spatial integrity measurements to be on the order of 2 mm. This level of accuracy is maintained during patient delivery by using the following procedure: setting up to an exhale breath-hold position and using a gating boundary around the region of interest that's 2 mm less than the PTV of interest (e.g., 3 mm expansion of the GTV if a 5-mm expansion to PTV). Depending on the location of the tumor (or other anatomy of interest), duty cycles so far have ranged from about 50% (especially for tumors close to diaphragm) to about 80% (for pancreatic lesions and other abdominal sites excluding liver). Examples are shown in figure below.

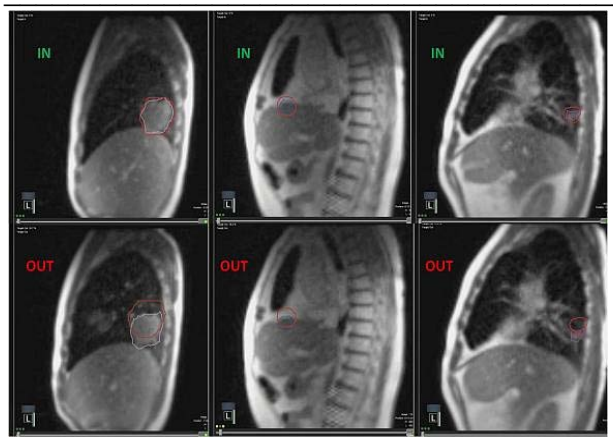

Conclusion: We have clinically demonstrated the practicality of real-time, real-anatomy tracking and have shown that clinical parameters can be selected which allow efficient treatment delivery. This work will be used as a foundation for evaluating options for treatment volume reduction.

PO-0892

Assessment of respiratory and cardiac motion to supplement MRI based tracking of hilar lymph nodes

L.P.W. Canjels[1], M.E.P. Philippens[1], T. Bruijnen[1], B. Stemkens[1], D.C.P. Cobben[1], S. Sharouni[1], J.J.W. Lagendijk[1], A.L.H.M.W. Van Lier[1], R.H.N. Tijssen[1]

[1]UMC Utrecht, Department of Radiation Oncology, Utrecht, The Netherlands

Purpose or Objective: In current radiotherapy for hilar or mediastinal lymph node metastases large treatment margins are used. Online MRI guidance will offer direct visualization of the lymph nodes, allowing highly conformal treatments using gating or tracking techniques. However, both respiratory and cardiac induced motion are expected to cause significant displacements. In this study we have assessed the relative contributions of the heart and respiration to the motion of hilar lymph nodes in order to find the optimal motion compensation strategy on the MR-Linac.

Material and Methods: Five healthy subjects were imaged during free-breathing using cine-MRI on a 1.5T MRI scanner. Sagittal and coronal scans, positioned through the center of the hilar lymph nodes, were acquired interleaved using a balanced Steady-State Free-Precession (bSSFP) sequence, providing T2/T1 contrast; Tacq = 1:08 min, TE/TR = 1.92/0.96 ms, 1.38 x 1.38 mm2, 7 mm slices, at a rate of 4 frames/sec. The motion in the region of the hilar lymph nodes was estimated using an optical flow algorithm [1]. As the cardiac induced motion manifests as a modulation of the respiratory motion waveform, power spectra were calculated to assess the relative contribution of each source of motion. The respiratory-to-cardiac power ratios were determined from the power spectrum by dividing the respiratory peak by the cardiac peak.

Results: Typical results of optical flow analysis on sagittal and coronal slices in Figs. 1A-B. Cardiac motion is shown to have significant contributions in left-right (LR) and anterior-posterior (AP) directions as shown by the power spectra (Fig. 1C). The mean lymph node displacements and respiratory-to-cardiac power ratios are listed in Table 1. The mean displacement was largest in CC direction. The respiratory-to-cardiac power ratio was largest in CC direction, while in LR direction the lowest values are observed. This implies that cardiac induced motion contributes most in LR direction, whereas respiratory induced motion dominates most in CC direction.

Conclusion: These preliminary results in five volunteers showed that cardiac motion has a significant contribution on the motion of hilar structures. This indicates that the cardiac component cannot be ignored when implementing motion compensation strategies. Soon, this study will start with the inclusion of lung cancer patients with lymph nodes metastases. The power spectra will be used to separate the cardiac from the respiratory signal to determine the exact cardiac induced displacement.

Tabel 1: Motion characteristics

	Craniocaudal direction		Left-Right direction		Anterior-posterior direction	
	Mean lymph node displacement (mm)*	respiratory-to-cardiac power ratio**	Mean lymph node displacement (mm)*	respiratory-to-cardiac power ratio**	Mean lymph node displacement (mm)*	respiratory-to-cardiac power ratio**
Subject 1	3.2	32	2.1	1.1	2.4	9.2
Subject 2	5.9	4.1	1.0	1.5	1.8	3.0
Subject 3	4.8	7.9	1.5	1.2	1.3	2.3
Subject 4	8.2	50	1.8	3.4	3.3	5.5
Subject 5	3.9	21	1.6	1.2	0.9	4.4
Average	5.2	23	1.6	1.8	1.9	4.4

* The mean lymph node displacement was calculated using a 95% confidence interval to exclude outliers
** The respiratory-to-cardiac power ratios were determined from the power spectrum by dividing the respiratory peak by the cardiac peak.

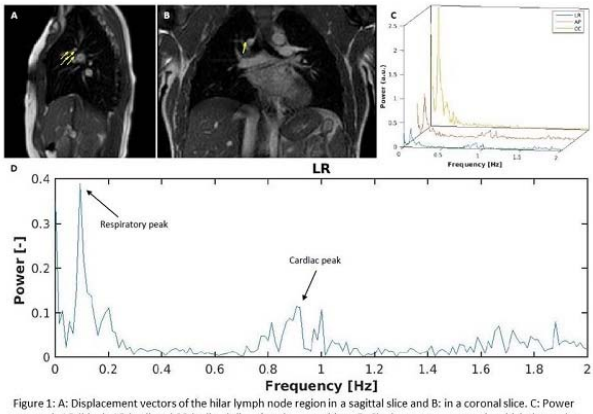

Figure 1: A: Displacement vectors of the hilar lymph node region in a sagittal slice and B: in a coronal slice. C: Power spectra in LR (blue), AP (red) and CC (yellow) directions in one subject. D: Single power spectrum in which the peaks used for the peak-to-peak ratio are indicated.

PO-0893

Direct comparison of electromagnetic guided couch and MLC tracking on a TrueBeam accelerator

R. Hansen[1], T. Ravkilde[1], E.S. Worm[1], J. Toftegaard[2], C. Grau[2], K. Macek[3], P.R. Poulsen[2]

[1]Aarhus University Hospital, Department of Medical Physics, Aarhus C, Denmark

[2]Aarhus University Hospital, Department of Oncology, Aarhus C, Denmark

[3]Varian Medical Systems, Imaging Laboratory, Baden, Switzerland

Purpose or Objective: Couch and MLC tracking are promising methods for real-time motion compensation for moving targets during radiation therapy. Couch and MLC tracking experiments have mainly been performed by different research groups, and no direct comparison of couch and MLC tracking of VMAT plans has been published. Varian TrueBeam 2.0 includes a prototype tracking system with selectable couch or MLC compensation. This study provides a direct comparison of the two tracking types with an otherwise identical setup.

Material and Methods: Several experiments were performed to characterize the geometric and dosimetric performance of electromagnetic guided couch and MLC tracking on a TrueBeam linear accelerator. The tracking system latency was determined without motion prediction as the time lag between sinusoidal target motion and the compensating motion of the couch or MLC as recorded by continuous MV portal imaging. The geometric and dosimetric tracking accuracy was measured in tracking experiments with motion phantoms that reproduced four prostate and four lung tumor trajectories. A Kalman filter was used for prediction in these experiments. The geometric tracking error in beam's eye view was determined as the distance between an embedded gold marker embedded and the circular MLC aperture in continuous MV images. The dosimetric tracking error was quantified as the Delta4-measured 2%/2mm gamma failure rate of a low and a high modulation VMAT plan delivered with the eight motion trajectories and using the static dose distribution as reference.